Mon. Not. R. Astron. Soc. **339,** 757–764 (2003)

H1320+551: a type 1.8/1.9 Seyfert galaxy with an unabsorbed X-ray spectrum

X. Barcons,* F. J. Carrera and M. T. Ceballos
Instituto de Física de Cantabria (CSIC-UC), 39005 Santander, Spain

Accepted 2002 October 23. Received 2002 September 24; in original form 2002 July 12

ABSTRACT

We present new optical spectroscopic and *XMM–Newton* X-ray observations of the active galactic nucleus (AGN) H1320+551. The optical data (consistent with but of better quality than a previously published spectrum) show this source to be a type 1.8/1.9 Seyfert galaxy at $z = 0.0653$. The narrow-line region is significantly reddened, with a Balmer decrement $\mathrm{H}\alpha/\mathrm{H}\beta \sim 6$, and the broad-line region, with a barely detectable Hβ broad component, shows a much pronounced Balmer decrement ($\mathrm{H}\alpha/\mathrm{H}\beta > 27$). In spite of this, the EPIC pn X-ray spectrum exhibits a power-law continuum with a soft excess that is well fitted by a blackbody, with no photoelectric absorption above the Galactic value. An Fe K emission line is also seen at a rest-frame energy ∼6.5 keV with an equivalent width of ∼400 eV, far too weak for the source to be Compton-thick. Reconciling the optical and X-ray data requires the narrow-line region to be internally reddened but with small covering factor over the nuclear emission, and the Balmer decrement of the broad-line region to be an intrinsic property rather than caused by reddening/absorption. The H1320+551 type 1.8/1.9 Seyfert galaxy is not consistent with being an obscured type 1 Seyfert nucleus, i.e. it does not match the basic AGN unified scheme hypothesis.

Key words: galaxies: active – galaxies: Seyfert – X-rays: galaxies.

1 INTRODUCTION

The X-ray spectral properties of active galactic nuclei (AGNs) are generally well correlated with their optical appearance. Type 1 Seyfert galaxies and quasi-stellar objects (QSOs) usually have steep X-ray spectra with little, if any, intrinsic photoelectric absorption (Nandra & Pounds 1994). Type 2 Seyfert galaxies have, in contrast, absorbed X-ray spectra (Smith & Done 1996). This is hardly surprising in the framework of the simplest version of the AGN unified model (Antonucci 1993), as the molecular gas and dust that prevents the direct view of the broad-line region (BLR) in type 2 Seyfert galaxies (the 'torus') is likely also to contain atomic gas that will absorb soft X-rays.

Unified AGN models for the cosmic X-ray background (XRB), first suggested by Setti & Woltjer (1989) and later worked out by Madau, Ghisellini & Fabian (1994), Comastri et al. (1995) and Gilli, Salvati & Hasinger (2001), make use of this feature. A broad distribution of photoelectric absorbing columns is assumed, which results in an integrated XRB with the required spectral shape. X-ray surveys are expected to reveal mostly type 1 AGNs for soft unabsorbed X-ray sources and type 2 AGNs for hard absorbed X-ray sources. Indeed, soft X-ray surveys carried out with *ROSAT* are rich in type 1 AGNs and QSOs [see, e.g., Mason et al. (2000) and Lehmann et al. (2001) for medium and deep *ROSAT* surveys]. On the contrary, hard X-ray surveys carried out with *BeppoSAX* do contain large numbers of type 2 AGNs (Fiore et al. 1999).

Risaliti, Maiolino & Salvati (1999) found that the X-ray absorption in a sample of [O III]-selected type 1.8, 1.9 and 2 AGNs reveals much higher absorbing columns than in samples selected by other means, a large fraction of the sources being actually Compton-thick. Since [O III] emission is supposed to arise above the obscuring torus, [O III] selection is likely to be an orientation-independent measure of the AGN intrinsic luminosity. Still, a rough trend of increasing X-ray absorption with AGN Seyfert type is found (Alonso-Herrero, Ward & Kotilainen 1997; Risaliti et al. 1999).

However, a number of studies show that the optical obscuration to X-ray absorption relation is not as simple as predicted by the AGN unified model. A hard spectrum selection of *ROSAT* X-ray sources, which was supposed to favour absorbed X-ray sources (Page, Mittaz & Carrera 2000), revealed mostly type 1 AGNs, while more type 2 AGNs were expected (Page, Mittaz & Carrera 2001). Granato, Danese & Franceschini (1997) proposed that X-ray absorption takes place mostly in dust-free regions, below the dust sublimation radius. This will accommodate the existence of X-ray absorbed, optically unobscured type 1 AGNs.

Pappa et al. (2001) have found, in a sample of type 2 Seyfert galaxies, some extreme cases without or with very small apparent

*E-mail: barcons@ifca.unican.es

intrinsic X-ray absorption. The apparent lack of X-ray absorption has been attributed to some of these type 2 Seyfert galaxies being actually Compton-thick, in which case we would be witnessing only scattered radiation and host galaxy emission from a circumnuclear starburst below 10 keV. Bassani et al. (1999) propose a three-dimensional diagnostic that would discriminate between that possibility and true lack of absorption, on the basis of a diagram displaying the equivalent width of the Fe K emission line versus the transmission T defined as the ratio between the 2–10 keV X-ray flux (supposed to measure the emission transmitted through the torus) and the reddening-corrected [O III] flux, assumed to measure the intrinsic AGN emission. Compton-thick type 2 AGNs lie invariably at the high-equivalent-width low-transmission end. That has helped to unmask a number of puzzling type 2 Seyfert galaxies apparently unabsorbed. The data quality of the *ASCA* spectra used by Pappa et al. (2001) was certainly good enough to discard a Compton-thick origin, but did not enable the discrimination between a dusty warm absorber and a genuine BLR-free AGN. Similar results have been obtained by Panessa & Bussani (2002) in a sample of 17 Seyfert 2 galaxies.

In this paper we present new optical and X-ray observations of H1320+551. This source was discovered by *HEAO-1* as part of the Modulation Collimator–Large Area Sky Survey (MC-LASS, Wood et al. 1984). The inferred 2–10 keV flux was $\sim 2 \times 10^{-11}$ erg cm^{-2} s^{-1} (Ceballos & Barcons 1996), although confusion could be an issue. Remillard et al. (1993) identified this X-ray source with a type 1 AGN at $z = 0.064$ (RA = $13^{\mathrm{h}}22^{\mathrm{m}}49\overset{\mathrm{s}}{.}2$, Dec. = $+54^{\circ}55'28''$). However, their optical spectrum was noisy and of poor spectral resolution ($\sim$10 Å) with a barely visible Hβ line.

H1320+551 was also detected in the *ROSAT* All-Sky Survey and identified in the *ROSAT* Bright Survey (Schwope et al. 2000). The *ROSAT* PSPC count rate was 0.23 ± 0.024 count s^{-1}, corresponding to an absorption-corrected 0.5–2 keV flux of $\sim(1.9 \pm 0.2) \times 10^{-12}$ erg cm^{-2} s^{-1}. The PSPC hardness ratio was $+0.12 \pm 0.10$. The source therefore had a moderately steep soft X-ray spectrum in the *ROSAT* band, but the small flux ratio $S(0.5\text{–}2)/S(2\text{–}10)$ (if the 2–10 keV flux was correct) suggested absorption. *ASCA* observed H1320+551 in 1999 May and we analyse the archival data here.

In what follows we present new optical spectroscopy and *XMM–Newton* X-ray observations of H1320+551. Our optical data (obtained in 1998) show this source to be a type 1.8/1.9 Seyfert galaxy at $z = 0.0653$ with a significantly reddened narrow-line region (NLR) (Section 2). The *XMM–Newton* X-ray spectrum is well described by a type-1-like continuum (power law plus blackbody) with no intrinsic photoelectric absorption, plus an Fe K emission-line complex (Section 4). In Section 5 we show that the unabsorbed X-ray spectrum is inconsistent with a dust-reddening origin for the large Balmer decrement in the broad-line region, which is instead more likely to be intrinsic to the broad-line clouds, contrary to the predictions of the AGN unified model.

2 OPTICAL OBSERVATIONS

H1320+551 was observed by the 4.2-m William Herschel Telescope (WHT) at the Observatorio del Roque de Los Muchachos on the island of La Palma (Canary Islands, Spain), on 1998 February 26. We used the ISIS double spectrograph with 600 line mm^{-1} gratings on both the blue and red arms, with the wavelengths centred at 5200 and 7000 Å, respectively, in order to observe the Hβ + [O III] region in the blue and the Hα + [N II] + [S II] in the red. During the second half of the night, when this observation was performed, the sky was clear and probably photometric. The seeing was $\sim$1.5 arcsec and we used a 1.5 arcsec slit width. Observations were carried out with the slit aligned to parallactic angle. Two exposures of 300 s each were taken. One of the blue spectra had a cosmic ray hit on top of the Hβ line and we have not used it. The two red-arm exposures were co-added.

Reduction and calibration were performed according to a standard sequence under the IRAF package. It included debiasing, flat-fielding, wavelength calibration with arc lamps, and flux calibration using a standard star and standard extinction curve for the observatory. The wavelength calibration gave residuals of 0.05 and 0.02 Å in the blue and in the red respectively. The measured spectral resolution (using Gaussian fits to unblended arc lines) gave 2.22 and 2.16 Å at the central wavelengths of the blue and red channels respectively. Given the relatively poor seeing, the spectrophotometric calibration is far from accurate, but certainly good to within a factor of 2.

Fig. 1 shows the resulting spectra in the blue and the red arms with marks on the most important lines. It is clear that the Hβ line is weak and dominated by a narrow component, with very weak, if any, broad component. The Hα + [N II] blend does, on the contrary, exhibit both a narrow and a broad Hα component. Therefore, according to the standard classification by Osterbrock (1989), the source is in principle a Seyfert 1.9. Remillard et al. (1993) classified it as a Seyfert 1 on the basis of a low spectral resolution ($\sim$10 Å) low signal-to-noise ratio optical spectrum (see fig. 3 in that paper). In

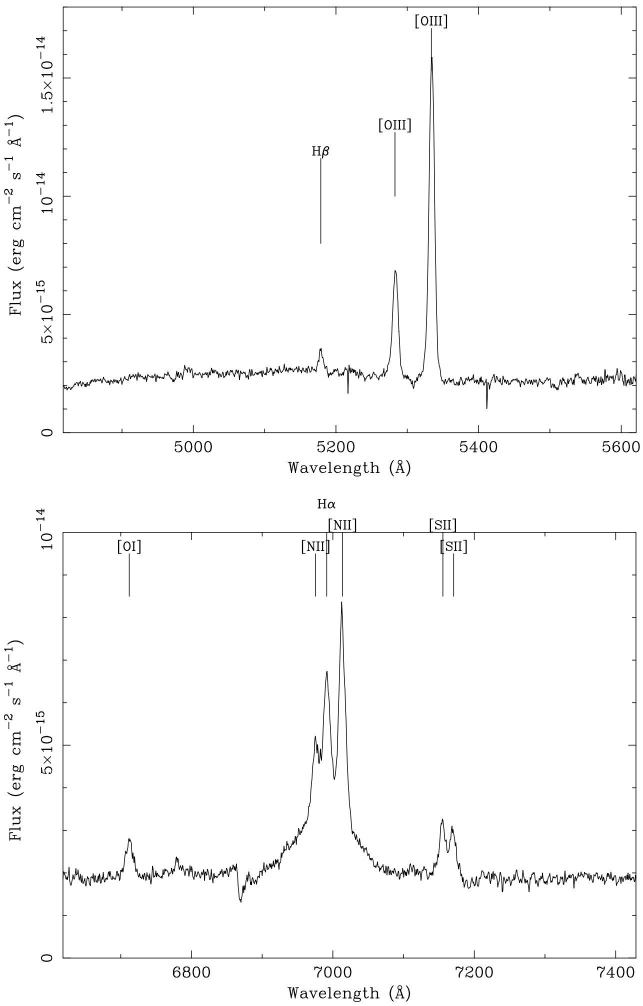

Figure 1. Optical spectrum of H1320+551, blue (top) and red (bottom) arms.

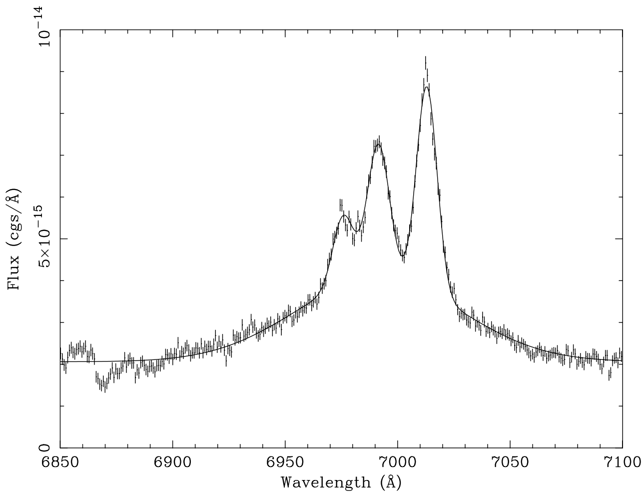

Figure 2. Detail of the optical spectrum and fit to the Hα + [N II] complex (see text for details).

their spectrum the Hβ line was barely visible and the Hα + [N II] complex could not be deblended.

In order to measure line intensities, we selected a small portion of the spectrum around each complex and we fitted the spectrum (via χ^2 minimization, using the QDP fitting routines) with a constant plus a Gaussian for each putative line. Errors on the intensity of each individual wavelength channel were propagated during the reduction process, in order to perform this fit correctly. The Hβ and each one of the [O III] doublet lines were fitted independently. The [S II] doublet, slightly blended, was fitted simultaneously with two Gaussians at the same redshift and with the same width. In the case of the Hα + [N II] blend, the three lines were simultaneously fitted to Gaussians, all of them with the same redshift and with the additional constraint that the two [N II] lines had the same width. An additional broad Hα line had to be added to achieve a good fit. The result is shown in Fig. 2. Based on the existence of a broad Hα component, we searched for a corresponding Hβ one with the same velocity width. This constrained fit yields a 'detection' of a weak broad Hβ component that is not required if the linewidth is left as a free parameter. This is the reason for the uncertainty in the 1.8/1.9 Seyfert type classification of this source.

Table 1 lists the measured line intensities and velocity widths (full width at half-maximum, FWHM). These were computed from the Gaussian fits, subtracting in quadrature the spectral resolution of the corresponding spectrograph channel (125 and 100 km s^{-1} in the blue and red arms respectively). The redshift that we fitted to the emission lines is $z = 0.065\,31 \pm 0.000\,02$, refining the value $z = 0.064$ reported by Remillard et al. (1993).

From the line intensities we see that this AGN has significant reddening. The Balmer decrement of the narrow-line region (NLR), as traced by the narrow-line components, is $(\mathrm{H}\alpha/\mathrm{H}\beta)_{\mathrm{NLR}} \sim 6$ (corresponding to $E(B - V) \sim 0.5$ mag), where $\sim$3 is expected for a variety of models under case B recombination and optically thin NLR gas. Narrow-line ratios can be reddening-corrected using the Balmer decrement as the indicator. Following Baldwin, Phillips & Terlevich (1981) we find log([O III]5007/Hβ4861) = 1.20 and log([N II]6583/Hα6562) = 0.145, which, as expected, place this object in the AGN zone in line diagnostic diagrams (e.g. Osterbrock 1989, fig. 12.1). We have further used the measured Balmer decrement from the narrow lines (Hα/Hβ $\sim$ 6), to estimate a gas column density of $N_{\mathrm{H}}(\mathrm{NLR}) \sim 3 \times 10^{21}$ cm^{-2}, assuming standard gas-to-dust ratio (Bohlin, Savage & Drake 1978).

Table 1. Measured line fluxes and velocity widths, as fitted to Gaussians. A velocity of 125 and 100 km s^{-1} has been subtracted in quadrature in the blue and red arm lines respectively, to account for the spectrograph resolution. The Hβ broad line has been fitted with the velocity fixed (*) at the value found for Hα, as otherwise this feature is not detected.

Line	Line flux ($\times10^{-15}$ erg cm^{-2} s^{-1})	FWHM (km s^{-1})
Hβ 4861 (narrow)	6.6	400
Hβ 4861 (broad)	6.7	3710*
[O III] 4958	45.5	525
[O III] 5007	130.4	500
[O I] 6300	13.5	520
[N II] 6548	19.1	450
Hα 6562 (narrow)	40.0	490
Hα 6562 (broad)	182.9	3710
[N II] 6583	56.4	450
[S II] 6716	15.7	445
[S II] 6730	14.4	445

Since the [O III] emission is likely to come from well above the torus, the intensity of the [O III]5007 line is supposed to be an orientation-independent estimator of the total AGN power. Following Bassani et al. (1999) and Pappa et al. (2001), who use the interstellar reddening law by Savage & Mathis (1979), we estimate the unreddened [O III]5007 flux by correcting the observed one by a factor $[(\mathrm{H}\alpha/\mathrm{H}\beta)_{\mathrm{NLR}}/3]^{2.94}$. The resulting [O III]5007 flux is $\sim 1.34 \times 10^{-12}$ erg cm^{-2} s^{-1}.

When a similar analysis is performed in the broad-line region (BLR), a Balmer decrement $(\mathrm{H}\alpha/\mathrm{H}\beta)_{\mathrm{BLR}} \sim 27$ is found. This should be considered as a lower limit, as the existence of an Hβ broad component (i.e. the type 1.8 Seyfert character of H1320+551) can only be established via constrained parameter fitting. If this Balmer decrement is interpreted in terms of reddening over a standard value of 3, a value of $E(B - V)_{\mathrm{BLR}} \sim 2$ mag is found, which for a standard dust-to-gas ratio corresponds to an H column density of $N_{\mathrm{H}}(\mathrm{BLR}) \sim 10^{22}$. In the framework of the AGN unified model, the difference between optical spectroscopic Seyfert types is due to an orientation effect which results in both reddening of the BLR and absorption of X-rays. Under these circumstances the above absorption column density should be seen in the X-ray data.

We have also tried to fit the broad-band optical spectra obtained here with a model mixing a reddened QSO, from the Francis et al. (1991) template, and an E/S0 galaxy template, from the Coleman, Wu & Weedman (1980) model. A good simultaneous description of the blue and red spectra is achieved with the QSO template, which can accommodate a very small amount of reddening, $E(B - V) <$ 0.1 mag, but it certainly needs some host galaxy light. The latter contributes about 40–60 per cent of the optical spectrum at our reference point at 5550 Å. Significantly larger reddening over the Francis et al. (1991) QSO template simply does not match the data. That suggests that whatever causes the large BLR Balmer decrement does not appear to be nuclear reddening.

3 PREVIOUS X-RAY OBSERVATIONS

3.1 *HEAO-1*

As already mentioned, X-ray emission from H1320+551 was discovered in the MC-LASS survey, which assigned it a count rate

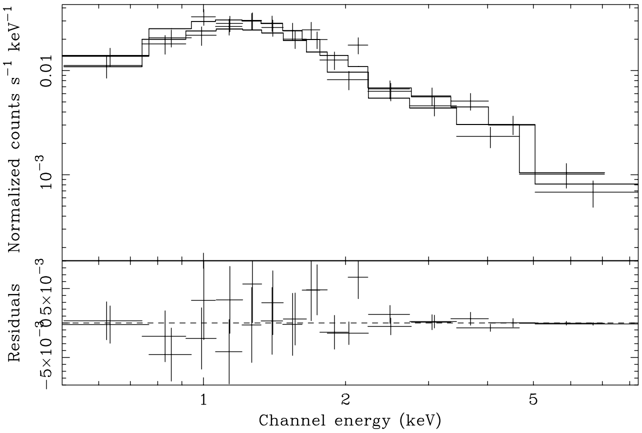

Figure 3. *ASCA* SIS0 and SIS1 spectrum of H1320+551 together with power-law fit plus Galactic absorption.

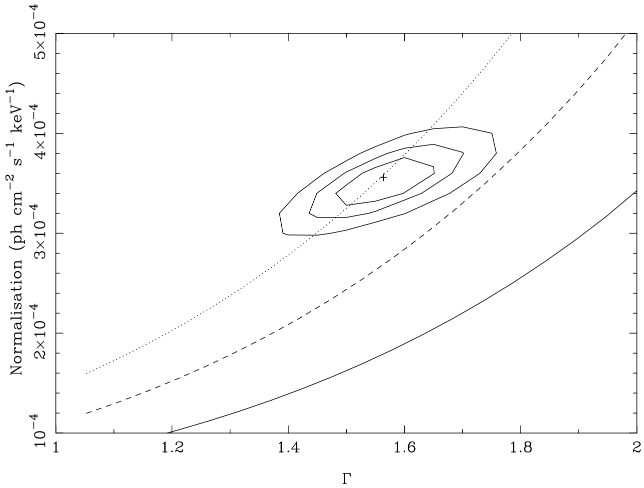

Figure 4. Confidence contours (1σ, 2σ and 3σ for two parameters) for the power-law index and normalization of the fit to the *ASCA* data for H1320+551. Lines at various 2–10 keV flux levels are also overlaid: 1.0 (continuous), 1.5 (dashed) and 2.0 (dotted) $\times 10^{-12}$ erg cm^{-2} s^{-1}.

of $(4.1 \pm 0.8) \times 10^{-3}$ count s^{-1}. Observations were carried out during 1977. Ceballos & Barcons (1996) assumed a $\Gamma = 1.7$ power-law spectrum and computed a 2–10 keV flux of 2.0×10^{-11} erg cm^{-2} s^{-1}.

3.2 *ROSAT*

H1320+551 was detected in the *ROSAT* All-Sky Survey (1990/91) as source 1RXS J 132248.5+545526 (Schwope et al. 2000) with a PSPC count rate of 0.23 ± 0.024 count s^{-1}, and a hardness ratio

$$\mathrm{HR}_{\mathrm{PSPC}} = \frac{C(0.5\text{–}2.0) - C(0.1\text{–}0.4)}{C(0.5\text{–}2.0) + C(0.1\text{–}0.4)} = 0.12 \pm 0.10,$$

where $C(0.1\text{–}0.4)$ and $C(0.5\text{–}2.0)$ are the PSPC counts collected in the 0.1–0.4 and 0.5–2.0 keV bands respectively. The 0.5–2.0 keV absorption-corrected flux was computed in Ceballos & Barcons (1996) by assuming a $\Gamma = 1.9$ power-law spectrum with Galactic absorption, resulting in $(1.9 \pm 0.2) \times 10^{-12}$ erg cm^{-2} s^{-1}.

3.3 *ASCA*

ASCA observed H1320+551 on 1999 May 10 for 10 ks. We have retrieved the pipeline-reduced data from the HEASARC public archive. The SIS0 and SIS1 data over the 0.5–8 keV band can be well fitted with a single power law with Galactic absorption, resulting in a $\chi^2 = 17.4$ for 26 degrees of freedom (see Fig. 3 for the *ASCA* spectrum). The data do not require additional absorption or a soft excess.

Fig. 4 shows the confidence contours for the power-law photon index ($\Gamma = 1.53 \pm 0.1$) and the normalization required by the *ASCA* data. We have also overlaid lines with various 2–10 keV flux levels, for comparison with the *XMM–Newton* observations. Indeed the *ASCA* 2–10 keV flux is 10 times smaller than the flux assigned to this source by the MC-LASS survey, although part of this discrepancy might be due to source confusion in the *HEAO-1* data.

4 *XMM–NEWTON* X-RAY OBSERVATIONS

H1320+551 was observed by *XMM–Newton* (Jansen et al. 2001) during revolution 366 on 2001 December 8. This observation was taken as part of the Guaranteed Time of the Survey Science Centre. The EPIC pn camera (Strüder et al. 2001) was operated in small-window mode with the 'Thin' filter. The MOS cameras (Turner et al. 2001) were operated in timing mode. The RGS spectrographs (den Herder et al. 2001) were operated in standard spectroscopy mode, but our target produced a very faint signal. Owing to the brightness of the source in the optical, the OM optical camera (Mason et al. 2001) was switched off during this observation. In this paper we present the analysis of the EPIC pn data only, as the Science Analysis Software (SAS) version 5.3.3 provides full support for calibration matrices of the small-window mode. The same version of the SAS is not meant to provide response matrices for the MOS cameras in timing mode.

The EPIC pn exposure time was 20 ks, with a count rate of 1.7 count s^{-1} in the 0.2–12 keV band. The background did not flare significantly during the observation. We used the EPIC pn calibrated event list provided in the pipeline products, which were obtained by processing the observation data file with SAS version 5.2. To gain full support in the analysis, we extracted the source and background spectrum, and generated redistribution matrices and ancillary response files using SAS version 5.3.3. The spectrum was also grouped in bins containing a minimum of 30 counts. All counts outside the 0.2–12 keV range were ignored.

As a first exercise, we computed the hardness ratios

$$\mathrm{HR}_1 = \frac{S(2.0\text{–}4.5) - S(0.5\text{–}2.0)}{S(2.0\text{–}4.5) + S(0.5\text{–}2.0)} \approx -0.681,$$

$$\mathrm{HR}_2 = \frac{S(4.5\text{–}12.0) - S(2.0\text{–}4.5)}{S(4.5\text{–}12.0) + S(2.0\text{–}4.5)} \approx -0.343.$$

These turn out to be entirely consistent with the average hardness ratios of the broad-line AGNs found in the AXIS medium-sensitivity survey: $\langle \mathrm{HR}_1 \rangle = -0.68 \pm 0.01$ and $\langle \mathrm{HR}_2 \rangle = -0.31 \pm 0.04$ (Barcons et al. 2002). The type 2 AGN in that survey have an average $\langle \mathrm{HR}_1 \rangle = -0.48 \pm 0.11$, which appears marginally harder than the values for H1320+551.

4.1 The 2–12 keV spectrum

We first fitted the 2–12 keV range with a single power law. We then checked for the existence of a (redshifted) Fe K line complex around 6–7 keV. A line was found at rest-frame energy of ~6.5 keV, with a very poorly defined intrinsic FWHM width of ~0.9 keV (see Table 2

Table 2. Best-fitting parameters for the X-ray spectrum of H1320+551 ($z = 0.0653$ assumed throughout). Parameters are grouped by model component, and the XSPEC routine used is also listed. Errors denote the 90 per cent interval for one parameter in each case. The best-fitting values and errors have been obtained by fitting the full 0.2–12.0 keV X-ray spectrum shown in the text, with the exception of the parameters labelled with *, which were obtained by fitting the 2–12 keV spectrum with a redshifted power law plus a Gaussian.

Parameter	Value
Photoelectric absorption: PHABS	
$N_{\rm H}$	$(1.69^{+0.45}_{-0.39}) \times 10^{20}$ cm^{-2}
Redshifted power law: ZPOWERLW	
Γ	1.87 ± 0.05
A_Γ	$(7.2^{+0.5}_{-0.3}) \times 10^{-4}$ photon cm^{-2} s^{-1}
Redshifted blackbody: ZBBODY	
kT	137^{+13}_{-12} eV
$A_{\rm BB}$	$(7.1_{-1.3}{}^{+1.4}) \times 10^{-6}$
Redshifted Fe K line complex: ZGAUSSIAN	
$E_{\rm line}{}^*$	6.51 ± 0.30 keV
$\sigma^*_{\rm line}$	$0.4^{+0.35}_{-0.4}$ keV
$F_{\rm line}$	$(10.5^{+3.7}_{-4.4}) \times 10^{-5}$ photon cm^{-2} s^{-1} keV^{-1}

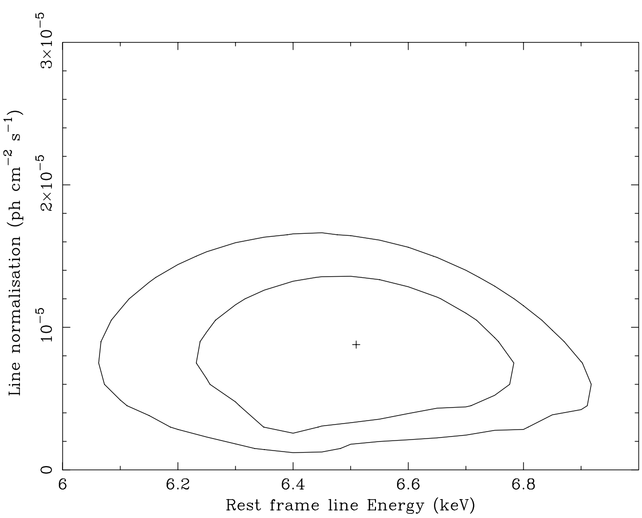

Figure 5. Confidence contours (1σ and 2σ) for the rest-frame Fe K line energy and intensity, following a Gaussian fit.

for the specific values). The significance of the line, as measured with the F-test statistic, is ~98 per cent. Confidence contours in the line rest-frame energy and line intensity parameter space are shown in Fig. 5. The corresponding equivalent width is $\sim 380^{+230}_{-320}$ eV in the rest frame. These parameters are roughly consistent with what is expected in Compton-thin type 2 Seyfert galaxies, where multiple components of the Fe K line might be present (see e.g. Iwasawa, Fabian & Matt 1997).

4.2 The soft excess and photoelectric absorption

When this fit is extrapolated to lower energies, a large soft excess becomes evident. We model this by adding a (redshifted) blackbody, and a local photoelectric absorption to account both for the Galactic one and any possible additional absorption in the source (note that we expect this to be $\sim 10^{22}$ cm^{-2} based on the Balmer decrement

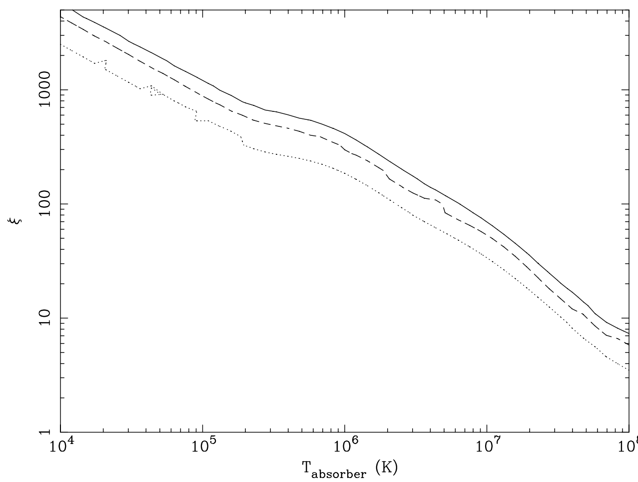

Figure 6. Limits for a $N_{\rm H} = 10^{22}$ cm^{-2} ionized absorber implied by the EPIC pn data: 1σ (continuous), 2σ (dashed) and 3σ (dotted).

of the BLR). The fit results in a $\chi^2 = 439.93$ for 413 degrees of freedom and a probability of the model not being able to describe the data of only 83 per cent. We tried to fit a plasma emission model (Raymond–Smith) instead of the blackbody, but no good fit could be achieved.

The rather high blackbody temperature ($kT_{\rm BB} \sim 140$ eV) suggests a low black hole mass $M_{\rm BH} \sim 10^4$–10^5 M$_\odot$, which is consistent with a luminosity of $\sim 3 \times 10^{43}$ erg s^{-1} from such a black hole radiating at near the Eddington limit.

It is remarkable that the fit to the X-ray data does not require any photoelectric absorption in excess of the Galactic value ($N_{\rm Gal} \sim 1.36 \times 10^{20}$ cm^{-2}). In fact we have frozen $N_{\rm H}$ to this value and added an extra photoelectric absorption component at the redshift of the target $z = 0.0653$. Refitting the data to this model finds its best value at no intrinsic absorption with a 3σ upper limit of 1.4×10^{20} cm^{-2}. This value is 70 times smaller than the minimum predicted from the BLR Balmer decrement interpreted in terms of dust reddening and for a normal gas-to-dust ratio. It is even seven times smaller than the value implied by the NLR reddening, but this might just be due to small covering factor of an internally reddened NLR.

The existence of an ionized absorber is ruled out by the X-ray data. The addition of a multiplicative ABSORI model with a fixed column density of $N_{\rm H} \sim 10^{22}$ cm^{-2} does not improve the χ^2. Only very large values of the ionization parameter $\xi > 1000$ or very high temperatures of the absorber ($kT \sim 10^8$ K) can reach a χ^2 as good as (but not smaller than) the one without an ionized absorber (see Fig. 6).

4.3 Resulting spectrum

Fig. 7 shows the resulting EPIC pn spectrum after the overall fit was performed, together with the contributions to the χ^2 from each channel. There are no residuals at the energies of the most prominent absorption edges. The existence of a slight positive residual at the hard energy end is uncertain as the background level is very high at these energies.

There is a negative residual at around 0.7 keV in the data (see Fig. 7). The feature extends for 0.1–0.2 keV with an amplitude of ~10 per cent. At the moment, individual calibration of the EPIC pn instrument gives residuals of ~3 per cent or less, but joint calibration of all *XMM–Newton* instruments leaves large discrepancies

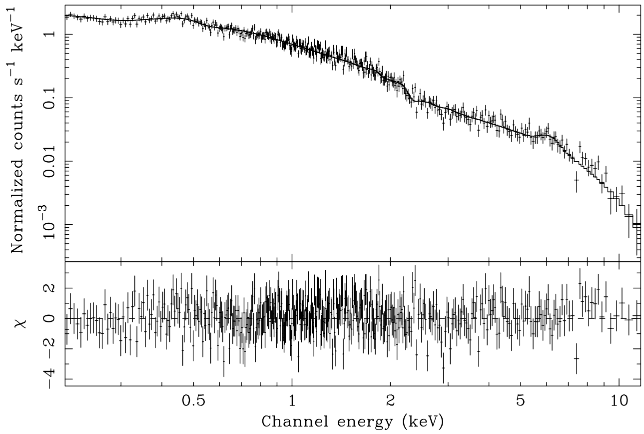

Figure 7. EPIC pn X-ray spectrum together with best-fitting model (top) and $\Delta\chi$ of data points to fitted model (bottom).

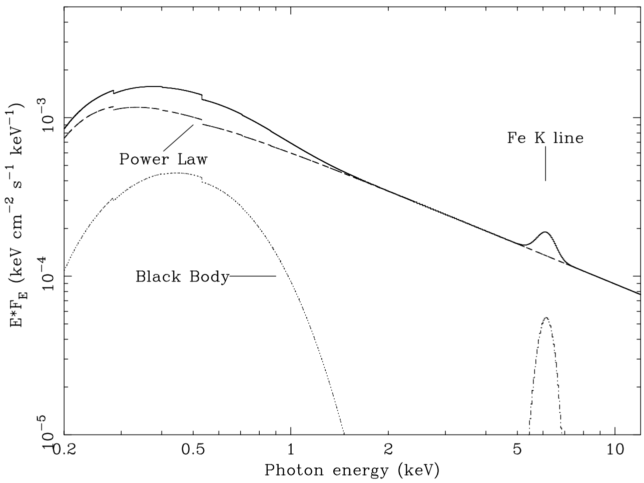

Figure 8. Fitted model, in terms of EF_E as a function of energy, showing the various components.

between EPIC pn and EPIC MOS in the energy range 0.3–1.3 keV of up to 15 per cent. Besides that, a negative residual similar to ours is seen in many EPIC pn spectra at around 0.7 keV (Sembay, private communication) and therefore we believe it to be a calibration artefact.

Fig. 8 shows the model fitted with the various components labelled. The flux, corrected for photoelectric absorption (assumed Galactic), of the source is $\sim 1.62 \times 10^{-12}$ erg cm^{-2} s^{-1} in the 0.5–2 keV band and 2.09×10^{-12} erg cm^{-2} s^{-1} in the 2–10 keV band. The luminosity is 3.1×10^{43} erg s^{-1} in the 0.5–2 keV band and 3.9×10^{43} erg s^{-1} in the 2–10 keV band. About 22 per cent of the 0.5–2 keV luminosity ($\sim 7 \times 10^{42}$ erg s^{-1}) is contributed by the soft excess that we have modelled as a blackbody, which is far too much to be attributable to the host galaxy or to scattering.

The fit to the X-ray spectrum is therefore typical of a type 1 Seyfert galaxy. There is an underlying power law, to which a soft excess, probably the direct quasi-thermal radiation from the accretion disc, has to be added. The Fe K emission-line complex is rather broad (FWHM $\sim$ 900 eV), as often found in type 2 Seyfert galaxies, for example in the prototypical NGC 1068 (as a result of the superposition of various components, Iwasawa et al. 1997). The equivalent width of the complex is 380^{+330}_{-320} eV, which lies in between the

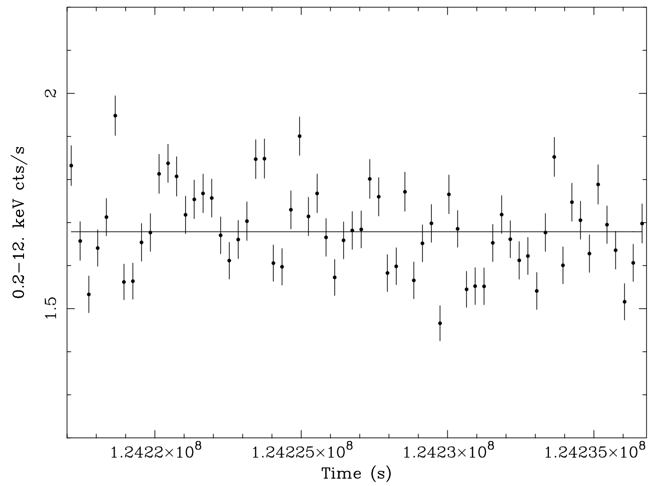

Figure 9. EPIC pn X-ray light curve, binned in 300 s bins. A constant fit is shown for comparison.

one expected from a Seyfert 1 and a Compton-thin Seyfert 2, all consistent with the Seyfert 1.8/1.9 nature of the source.

4.4 Source variability

In order to gain further insight into the X-ray properties of this X-ray source, we have extracted its EPIC pn light curve. Time intervals have been binned in 300 s, resulting in a signal-to-noise ratio of $\sim$18. The background counts have been estimated from the same background subtraction region that was used to analyse the spectrum. The resulting 0.2–12 keV light curve is shown in Fig. 9.

The average count rate is 1.67 count s^{-1}. However, the light curve is not consistent with a constant flux. A first glance at Fig. 9 reveals that two-thirds of the properly computed 1σ error bars do not cross the horizontal fit, while only one-third would be expected. The χ^2 of the fit to a constant intensity is extremely poor, $\chi^2/\nu = 341/65$.

To estimate the rms variability, we compare the measured variance of the count rates to the variance expected from the error bars and find 5 per cent intrinsic variability on that time-scale. Although small, these variations are highly significant. Note that for a 10^5 M$_\odot$ black hole, variability is expected down to scales of seconds.

The fact that the source varies brings additional support to the rejection of a Compton-thick model, which would not predict short-term variability.

5 DISCUSSION

Reconciling the Seyfert 1.8/1.9 character of H1320+551, as drawn from the optical observation in 1998, with the *XMM–Newton* data, taken late 2001, has two possible scenarios. The first one is that the source spectrum changes over time. It would then be possible that both the optical and X-ray absorbing properties change simultaneously. The other possibility is that both the optical and the X-ray properties derived from the 1998 optical data and the 2001 *XMM–Newton* X-ray observation stay constant over time. In that case we find that H1320+551 is not consistent with a type 1 Seyfert AGN viewed through absorbing material.

5.1 Does the H1320+551 spectrum vary?

The first issue to address is whether the various data sets give a consistent picture of H1320+551 or there is rather strong evidence for varying spectral properties. As already discussed, the optical spectrum presented here is of superior quality to that of Remillard et al. (1993), and therefore we do not believe there is a strong case for claiming a change in optical spectral type from Seyfert 1 to Seyfert 1.8/1.9 by comparing the two spectra.

The *HEAO-1* data give a flux that is ~10 times larger in the 2–10 keV band than any other reported flux in that band. Although it is entirely possible that the *HEAO-1* flux was correct (therefore implying a large variation after two decades), this flux might have been severely contaminated by other sources within the same field of view of the Modulation Collimator. To assess this point further, we have searched for RASS sources in the vicinity of H1320+551, and found a total of nine sources within a radius of 2 deg, totalling a flux ~5 times that of our target. Although this does not prove that the *HEAO-1* flux is wrong, it illustrates the difficulty in avoiding confusion problems in the MC-LASS fluxes.

The *ROSAT* All-Sky Survey measurement is entirely consistent with the *XMM–Newton* one. The 0.5–2 keV flux measured in the RASS [$(1.9 \pm 0.2) \times 10^{-12}$ erg cm^{-2} s^{-1}] is consistent, within errors, with the 0.5–2 keV flux measured in the EPIC spectrum (1.6×10^{-12} erg cm^{-2} s^{-1}). Furthermore, we have folded the best-fitting *XMM–Newton* model through the PSPC-B response and found an expected PSPC hardness ratio of +0.15, while 0.12 ± 0.10 was measured. The spectral shapes of H1320+551, as seen in the *ROSAT* and *XMM–Newton* observations, are entirely consistent.

The *ASCA* data give a 2–10 keV flux very similar to the *XMM–Newton* one, but with no soft excess visible. In fact the underlying power law in the *ASCA* data is flatter than the *XMM–Newton* one, with the net result that, within uncertainties, *ASCA* finds a harder spectrum than *XMM–Newton*. To assess that point further, we simulated the *ASCA* spectrum with the model fitted to *XMM–Newton*. A single power law with no absorption gives a fairly acceptable fit ($\chi^2 = 36.25$ for 26 degrees of freedom) but the power-law index is significantly steeper ($\Gamma = 2.0 \pm 0.1$) than the one measured in the real *ASCA* data ($\Gamma = 1.5 \pm 0.1$). That discrepancy looks far too large to be attributable to cross-calibration errors, which are likely to be much smaller between EPIC pn and *ASCA* SIS (Snowden 2002). The fluxes measured in the fake *ASCA* data are 1.5 and 1.7×10^{-12} erg cm^{-2} s^{-1} in the 0.5–2 keV and 2–10 keV bands respectively, while 0.7 and 1.65×10^{-12} erg cm^{-2} s^{-1} result from the best power-law fit to the real *ASCA* data. While there is agreement in the 2–10 keV band, the soft excess seen in the *XMM–Newton* observation, consistently with the earlier *ROSAT* observation, is not seen in the *ASCA* data.

Therefore there is some marginal evidence for X-ray spectral changes in H1320+551. Whether that implies changing absorption properties is unclear, and cannot be addressed with the archival *ASCA* observations confronted to the *XMM–Newton* and earlier *ROSAT* ones.

5.2 An intrinsic Balmer decrement

If the WHT and *XMM–Newton* data presented here are representative of the true average state of H1320+551, there is an apparently contradictory behaviour in the optical and in X-rays. The large Balmer decrement seen in the BLR is not consistent with the unabsorbed X-ray spectrum, if both phenomena have to be explained in terms of reddening/absorption.

Pappa et al. (2001) have studied a sample of eight type 2 Seyfert galaxies, where they find at least two without photoelectric absorption in X-rays. Three explanations were proposed in that work to account for the unusual behaviour of these sources: (a) the lack of BLR is real and intrinsic to the nuclear properties; (b) the type 2 Seyfert galaxies are Compton-thick, in which case the apparent lack of photoelectric absorption would be due to the <10 keV flux coming only from scattered and/or host galaxy emission; and (c) the presence of a dusty warm absorber reddens the BLR but has little effect in the X-ray properties. Indeed with the *ASCA* spectra of these objects, Pappa et al. were unable to find spectral features associated to the warm absorber.

We have carefully examined these three possibilities in the case of H1320+551. There are two independent reasons to rule out a Compton-thick scenario (b). First we use the three-dimensional diagnostic diagram proposed by Bassani et al. (1999). For H1320+551 the transmission is $T \sim 1.5$ and the equivalent width of the Fe K line is ~400 eV. Both numbers are inconsistent with a Compton-thick source; instead H1320+551 would be consistently placed in between Seyfert 1 and Compton-thin Seyfert 2, which is what would be expected for a Seyfert 1.8/1.9. A second independent fact rejecting a Compton-thick scenario comes from the detection of X-ray variability on scales of 300 s. If the X-rays detected from H1320+551 were due to scattered radiation, the variability scale would be associated to the reflector rather than to the nuclear source and it would be much longer.

The possibility of a dusty warm absorber (c) is also excluded from the X-ray analysis presented here. No spectral features are detected in the X-ray data, and in fact any absorbing gas present should be fully ionized, something rather inconsistent with the presence of dust reddening the BLR.

That leaves the intrinsic origin (a) for the large BLR decrement as the only likely explanation. This assumption is at odds with the standard AGN unified model and deserves some further discussion. In what follows we address the question on whether H1320+551 is consistent with an absorbed/reddened type 1 Seyfert or not.

Ward et al. (1988) studied the Balmer decrement of type 1 AGNs in the Piccinotti et al. (1982) sample. The good linear correlation between Balmer decrement versus the ratio between 2–10 keV luminosity (mostly unaffected by reddening/absorption) and Hβ luminosity (a good tracer of absorption) prompted Ward et al. (1988) to suggest that Balmer decrement is determined by nuclear reddening, rather than being intrinsic to the BLR (see their fig. 4). They also find an approximately constant 2–10 keV to Hα ratio for the sample (see their fig. 5). In fact, Ward et al. (1988) conclude that, in spite of the extreme conditions of the BLR, the intrinsic Balmer decrement is ~3.5 for the type 1 AGNs.

Now, H1320+551 has a Balmer decrement that is more than half a decade larger than what would be expected from its 2–10 keV to Hβ ratio. Reddening correction will not bring this into agreement with the type 1 Seyfert galaxies, as both the Balmer decrement and the X-ray to Hβ ratio will decrease if reddening-corrected. On the contrary, the 2–10 keV to Hα ratio is entirely consistent with that of type 1 Seyfert galaxies. All that means that the large BLR decrement for this particular Seyfert 1.8/1.9, together with its unabsorbed X-ray spectrum, cannot be explained as a Seyfert 1 AGN viewed through obscuring material.

6 CONCLUSION

XMM–Newton X-ray observations of the H1320+551, which is classified by its optical spectrum as a type 1.8/1.9 AGN, reveal no absorption. If the non-simultaneous optical and X-ray observations both trace the true state of this source, we conclude that the large Balmer decrement of the BLR, which determines its 1.8/1.9 spectroscopic type, is not due to reddening by dusty absorbing material along the line of sight. A variety of models can explain a large intrinsic value of the Balmer decrement, among them the failure of the standard 'case B recombination' and/or optically thick BLR clouds. In any case, the AGN unified model fails completely in this source.

Regardless of whether the unusual optical/X-ray absorption properties of H1320+551 are due to variations or not, they raise an important issue for unified AGN models for the X-ray background. H1320+551 is a source with a relatively soft unabsorbed X-ray spectrum that is expected typically to have a type 1 AGN optical counterpart. However, we identify it with a Seyfert 1.8/1.9, breaking again the one-to-one identification between X-ray absorption and optical obscuration that the XRB models use. Similarly, other relatively soft X-ray sources with no X-ray absorption might have optical counterparts which deviate from the standard Seyfert 1 character. If the BLR properties are not always linked to the absorption displayed by AGN, then Seyfert 1.8/1.9/2 galaxies might appear as optical counterparts of soft X-ray selected sources as well as type 1 Seyfert galaxies often appear as optical counterparts to hard X-ray sources.

ACKNOWLEDGMENTS

The work reported herein is based partly on observations obtained with *XMM–Newton*, an ESA science mission with instruments and contributions directly funded by ESA member states and the USA (NASA).

We are grateful to Steve Sembay and Martin Turner for help with EPIC calibration issues. The referee is also thanked for important suggestions on the original version of this paper. The WHT telescope is operated on the island of La Palma by the Isaac Newton Group of Telescopes in the Spanish Observatorio del Roque de Los Muchachos of the Instituto de Astrofísica de Canarias. Partial financial support for this work was provided by the Spanish Ministry of Science and Technology under project AYA2000-1690.

REFERENCES

Alonso-Herrero A., Ward M. J., Kotilainen J. K., 1997, MNRAS, 288, 977
Antonucci R., 1993, ARA&A, 31, 473
Baldwin J. A., Phillips M. M., Terlevich R. J., 1981, PASP, 93, 5
Barcons X., Carrera F. J., Watson M. G. et al., 2002, A&A, 382, 522
Bassani L., Dadina M., Maiolino R., Salvati M., Risaliti G., Della Ceca R., Matt G., Zamorani G., 1999, ApJ, 121, 473
Bohlin R. C., Savage B. D., Drake J. F., 1978, ApJ, 224, 132
Branduardy-Raymont G., Sako M., Kahn S. M., Brinkman A. C., Kaastra J. S., Page M. J., 2001, A&A, 365, L140
Ceballos M. T., Barcons X., 1996, MNRAS, 282, 493
Coleman G. D., Wu C. C., Weedman D. W., 1980, ApJS, 43, 393
Comastri A., Setti G., Zamorani G., Hasinger G., 1995, A&A, 296, 1
den Herder J. W. et al., 2001, A&A, 365, L7
Fiore F., La Franca F., Giommi P., Elvis M., Matt G., Comastri A., Molendi S., Gioia I., 1999, MNRAS, 306, L55
Francis P. J., Hewett P. C., Foltz C. B., Chafee F. H., Weymann R. J., Morris S. L., 1991, ApJ, 373, 465
Gilli R., Salvati M., Hasinger G., 2001, A&A, 366, 407
Granato G. L., Danese L., Franceschini A., 1997, MNRAS, 486, 147
Iwasawa K., Fabian A. C., Matt G., 1997, MNRAS, 289, 443
Jansen F. A. et al., 2001, A&A, 365, L1
Lee J. C., Ogle P. M., Canizares C. R., Marshall H. L., Schulz N. S., Morales R., Fabian A. C., Iwasawa K., 2001, ApJ, 554, L13
Lehmann I., Hasinger G., Schmidt M. et al., 2001, A&A, 371, 833
Madau P., Ghisellini G., Fabian A. C., 1994, MNRAS, 270, L17
Mason K. O., Carrera F. J., Hasinger G. et al., 2000, MNRAS, 311, 456
Mason K. O. et al., 2001, A&A, 365, L36
Nandra K., Pounds K. A., 1994, MNRAS, 268, 405
Osterbrock D. E., 1989, Astrophysics of Gaseous Nebulae and Active Galactic Nuclei. University Science Books, Mill Valley, CA
Page M. J., Mittaz J. P. D., Carrera F. J., 2000, MNRAS, 318, 1073
Page M. J., MIttaz J. P. D., Carrera F. J., 2001, MNRAS, 325, 575
Panessa F., Bussani L., 2002, A&A, 394, 435
Pappa A., Georgantopoulos I., Stewart G. C., Zezas A. L., 2001, MNRAS, 326, 995
Piccinotti G., Mushotzky R. F., Boldt E. A., Holt S. S., Marshall F. E., Serlemitsos P. J., Shafer R. A., 1982, ApJ, 253, 485
Remillard R. A., Bradt H. V., Brissenden R. J. V., Buckley D. A. H., Roberts W., Schwartz D. A., Stroozas B. A., Tuohy I. R., 1993, AJ, 105, 2079
Risaliti G., Maiolino R., Salvati M., 1999, ApJ, 522, 157
Savage B. D., Mathis J. S., 1979, ARA&A, 17, 73
Schwope A. D., Hasinger G., Lehmann I. et al., 2000, Astron. Nachr., 321, 1
Setti G., Woltjer L., 1989, A&A, 224 L21
Smith D., Done C., 1996, MNRAS, 280, 355
Snowden S., 2002, in Jansen F. A., ed., New Visions of the X-ray Universe in the XMM–Newton and Chandra Era. ESA, Noordwijk, in press
Strüder L. et al., 2001, A&A, 365, L18
Turner M. J. L. et al., 2001, A&A, 365, L27
Ward M. J., Done C., Fabian A. C., Tennant A. F., Shafer R. A., 1988, ApJ, 324, 767
Wood K. S., Meekins J. F., Yentis D. J. et al., 1984, ApJS, 56, 507

This paper has been typeset from a TEX/LATEX file prepared by the author.